JACS
JOURNAL OF THE AMERICAN CHEMICAL SOCIETY
Article
pubs.acs.org/JACS

Do π-Conjugative Effects Facilitate S_N2 Reactions?

Chia-Hua Wu,[†] Boris Galabov,*[,‡] Judy I-Chia Wu,*[,†] Sonia Ilieva,[‡] Paul von R. Schleyer,[†] and Wesley D. Allen*[,†]

[†]Center for Computational Chemistry and Department of Chemistry, University of Georgia, Athens, Georgia 30602, United States
[‡]Department of Chemistry, University of Sofia, Sofia 1164, Bulgaria

Supporting Information

ABSTRACT: Rigorous quantum chemical investigations of the S_N2 identity exchange reactions of methyl, ethyl, propyl, allyl, benzyl, propargyl, and acetonitrile halides (X = F^-, Cl^-) refute the traditional view that the acceleration of S_N2 reactions for substrates with a multiple bond at C_β (carbon adjacent to the reacting C_α center) is primarily due to π-conjugation in the S_N2 transition state (TS). Instead, substrate−nucleophile electrostatic interactions dictate S_N2 reaction rate trends. Regardless of the presence or absence of a C_β multiple bond in the S_N2 reactant in a series of analogues, attractive $C_\beta(\delta^+)\cdots X(\delta^-)$ interactions in the S_N2 TS lower net activation barriers (E^b) and enhance reaction rates, whereas repulsive $C_\beta(\delta^-)\cdots X(\delta^-)$ interactions increase E^b barriers and retard S_N2 rates. Block-localized wave function (BLW) computations confirm that π-conjugation lowers the net activation barriers of S_N2 allyl (**1t**, coplanar), benzyl, propargyl, and acetonitrile halide identity exchange reactions, but does so to nearly the same extent. Therefore, such orbital interactions cannot account for the large range of E^b values in these systems.

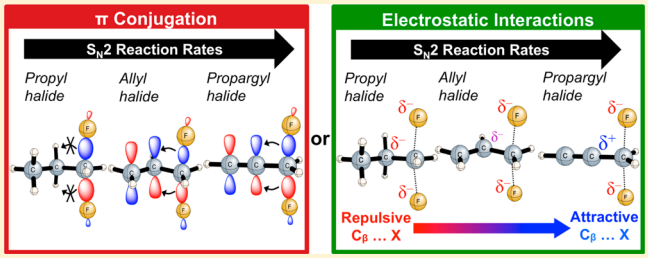

INTRODUCTION

The rates of bimolecular nucleophilic substitution (S_N2) reactions often are enhanced when a multiple bond is present at the β position adjacent to the reaction center. Traditionally, S_N2 rate enhancements of this type, such as the "allylic" and "benzylic" effects, have been attributed to "the ability of the multiple bond to delocalize the developing negative charge at the reaction site."[1] In this explanation, favorable conjugative delocalization from the C_α−LG (leaving group) and C_α−Nu (nucleophile) bonds to the substrate π orbitals (Figure 1)

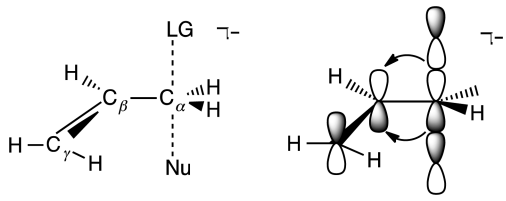

Figure 1. Conventional view of the allylic effect, in which $\sigma \rightarrow \pi^*$ conjugation between the $\sigma(C_\alpha\text{–LG})/\sigma(C_\alpha\text{–Nu})$ (LG = leaving group, Nu = nucleophile) bonds and substrate π orbitals stabilizes the S_N2 transition state.

stabilizes S_N2 transition states (TS) and yields faster S_N2 rates. Accordingly, Ingold claimed sixty years ago that "in aralphyl compounds containing alpha-phenyl substituents, the more powerful mechanism of conjugative electron displacements is available to assist the separation of the displaced group; and a formed carbonium ion is stabilized by conjugative mesomerism."[2] Here we examine the validity of this conventional viewpoint.

Allylic and benzylic effects are apparent in the average 1:40:120 S_N2 reaction rate ratios observed for ethyl, allyl, and benzyl halides in various organic solvents.[3] In acetone, 1-chloro-2-butene reacts with potassium iodide 630 times faster than does *n*-butyl chloride;[4] other cases are documented.[5] That the S_N2 reaction rate of $(PhCH_2)_2SEt^+$ is 8000 times faster than that for 2-ethyl-3,4-dihydro-1*H*-2-benzothiopyranium was attributed to the relative orientation of the S_N2 reaction center in the latter, which precludes π-conjugation with the adjacent aromatic ring.[6] Substrates with triple bonds at the β position also display accelerated S_N2 rates as compared to their saturated counterparts.[4] Nevertheless, is π-conjugation between the C_α−LG/C_α−Nu bonds and substrate π orbitals the actual cause of faster S_N2 reaction rates for substrates with multiple bonds?

While the conventional explanation for the allylic and benzylic effect is appealing, there is evidence that this view is at least incomplete if not inaccurate. On the basis of both FT-ICR experiments and electronic structure theory, Brauman and co-workers[7,8] showed that inherent electrostatics rather than π-conjugation is the driving force for fast S_N2 reactions of benzylic systems and chloroacetonitrile. Semiempirical computations[7] indicate that several benzyl halide S_N2 transition states and corresponding reactant and product complexes have quite similar resonance stabilization. As in the chloroacetonitrile

Received: November 1, 2013
Published: January 22, 2014

   dx.doi.org/10.1021/ja4111946 | J. Am. Chem. Soc. 2014, 136, 3118−3126

case,[8] no significant charge transfer occurs from the S_N2 reaction center to the benzylic π system as the reaction proceeds.

In contrast, the S_N2 activation barriers of various RCH_2X substrates (R = $CH{=}CH_2$, $C{\equiv}CH$, and $C{\equiv}N$) correlate inversely with their π-electron accepting abilities,[9,10] as expected from the traditional understanding of the allylic effect. From a different perspective, Streitwieser et al.[11] proposed that polarization of the allylic π bond toward the TS could be responsible for the S_N2 allylic effect. However, a comprehensive computational study of S_N2 identity exchange reactions of allylic systems concluded the opposite.[12] In particular, both electronegative nucleophiles/leaving groups and π electron-withdrawing substituents decrease the net activation barrier; that is, polarization of substrate π bonds away from the TS reaction center leads to increased S_N2 reactivity.

Investigations of gas-phase S_N2 processes have long been used to expose intrinsic reactivities devoid of solvation effects. These fundamental S_N2 reactions feature a double-well potential energy surface.[13] As shown in Figure 2 for general

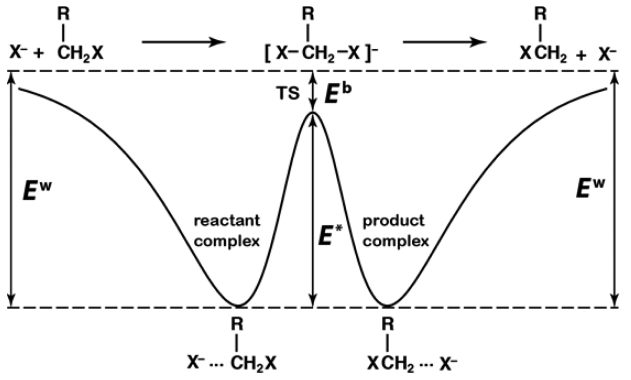

Figure 2. Schematic potential energy surface for gas-phase S_N2 identity exchange reactions.

S_N2 identity halide exchange, a reactant complex between the substrate ($R{-}CH_2X$) and nucleophile (X^-) forms first. After passing through the TS, a product complex precedes the dissociation of the leaving group. The key energetic quantities for S_N2 reactions are defined in Figure 2. E^w is the binding energy of the reactants; E^* is the internal barrier separating the reactant and product complexes via the TS; and E^b, the net activation energy, is the difference between the energies of the TS and the separated reactants. Prior studies[14,15] have established that E^b rather than E^* values quantify gas-phase S_N2 reactivities most accurately.[16] More negative/positive E^b values imply faster/slower S_N2 reaction rates.

The high-level focal-point analysis (FPA) computations of Galabov et al.[14] established the E^b energies for the S_N2 identity exchange reactions of benzyl fluoride, benzyl chloride, and several *para*-substituted derivatives. Natural bond orbital (NBO) populations indicated that "the delocalization of nucleophilic charge into the aromatic ring in the S_N2 transition states is quite limited and should not be considered the origin of benzylic accelerations of S_N2 reactions."[14] Instead, a remarkable linear dependence was found between E^b values of a series of benzylic S_N2 reactions and the electrostatic potentials at the reaction center carbons. The resulting conclusion was that "the critical effect of the aromatic ring in benzylic S_N2 systems is to raise the electrostatic potential surrounding the reaction center carbon atom." Recently, Rawlings et al.[17] questioned the completeness of this explanation based on a vinylogue extrapolation (VE) method and block localized wave functions (BLW),[18−20] claiming that "π delocalization is a significant contributor to the benzylic effect."

Our study unravels the S_N2 allylic/benzylic effect by rigorous computations on a broad sample of identity exchange reactions involving ethyl, methyl, propyl, allyl, benzyl, propargyl, and acetonitrile halides. The following questions are addressed: Is the conventional π-conjugation interpretation[11,12,14] for the allylic/benzylic effect correct? If not, what is the role and extent of such π-conjugative assistance in S_N2 transition states? What other factors influence the S_N2 rates of allylic and benzylic systems? The computational investigation presented herein, employing state-of-the-art quantum mechanical treatments, the FPA approach,[15,21−26] computed electrostatic potentials and NBO charges[27−29] at key sites in the TS, the BLW method,[18−20] and the activation strain (AS) model,[30,31] gives comprehensive answers to these questions. For some of the systems studied here, E2 or S_N2' mechanisms might be competitive;[32−36] nevertheless, to keep the scope of the investigation manageable, we do not analyze such alternative reactions.

METHODS

Geometry optimizations were performed for S_N2 identity exchange reactions with the CCSD(T) method[37−41] and aug′-cc-pVTZ basis set,[42−44] as well as B3LYP density functional theory[45−47] paired with a DZP++ basis set.[14,15,24,48] The S_N2 systems studied included $R{-}CH_2F + F^-$ ($R{-}CH_2$ = ethyl, propyl, methyl, allyl, propargyl, acetonitrile), $R{-}CH_2Cl + Cl^-$ ($R{-}CH_2$ = propyl, allyl, propargyl), substituted allyl fluorides $Y{-}CH{=}CHCH_2F + F^-$ (Y = CH_3, OCH_3, F, Cl, $CH{=}CH_2$, $C{\equiv}CH$, $C{\equiv}N$, CHO, NO_2), and substituted propyl fluorides $Y{-}CH_2CH_2CH_2F + F^-$ (Y = H, F, Cl, CH_3, CN, CCH, CHO, $CHCH_2$, OCH_3, NO_2). Aug′-cc-pVTZ refers to a hybrid atomic-orbital Gaussian basis set comprised of aug-cc-pVTZ (with diffuse functions) for the anionic $-C_\alpha H_2X_2^-$ reacting fragment and cc-pVTZ for the remaining atoms. The Supporting Information (Figure S1) documents insignificant differences between CCSD(T)/aug′-cc-pVTZ and CCSD(T)/aug-cc-pVTZ optimized geometric structures for the parent $CH_2{=}CHCH_2F + F^-$ system. Vibrational frequencies and zero-point vibrational energies (ZPVEs) were computed at the MP2[49]/aug′-cc-pVTZ level of theory. All CCSD(T) and MP2 analytic gradient computations were performed with CFOUR[50] or Molpro v2010.[51]

Focal point analyses[15,21−26] at CCSD(T)/aug′-cc-pVTZ optimized structures established the E^w, E^*, and E^b values for the S_N2 identity exchange reactions. Unless otherwise stated, E^w and E^b were computed with respect to the lowest-energy conformer of the reactant. Conformational details of the allyl fluoride S_N2 reaction pathways are provided in the Supporting Information (Figure S2). Restricted Hartree−Fock (RHF) and MP2 energies with full aug-cc-pVXZ (X = D, T, Q, 5) basis sets[42−44,52] were utilized for complete basis set (CBS) extrapolations by means of customary functional forms:[53,54]

$$E_n^{HF} = E_{CBS}^{HF} + a\, e^{-bn} \quad (n = 3, 4, 5) \tag{1}$$

and

$$\varepsilon_n^{MP2} \equiv E_n^{MP2} - E_n^{HF} = \varepsilon_{CBS}^{MP2} + bn^{-3} \quad (n = 4, 5) \tag{2}$$

Taking advantage of basis set additivity for high-order electron correlation, CCSD(T) energies at the CBS limit were evaluated with a composite (c∼) approximation:

$$E_{c\sim CBS}^{CCSD(T)} = E_{CBS}^{HF} + \varepsilon_{CBS}^{MP2} + E_{aug\text{-}cc\text{-}pVQZ}^{CCSD(T)} - E_{aug\text{-}cc\text{-}pVQZ}^{MP2} \tag{3}$$

dx.doi.org/10.1021/ja4111946 | J. Am. Chem. Soc. 2014, 136, 3118−3126

Final FPA results were obtained by appending CCSD(T)/c∼CBS energies with CCSD(T)/aug-cc-pCVTZ core electron correlation corrections and the aforementioned ZPVEs. The single-point energies for the FPA computations were obtained with Molpro v2010,[51] except for MP2/aug-cc-pV5Z cases whose size demanded use of the MPQC 2.3 program.[55] For interpretive purposes, electrostatic potentials at the atomic centers[56−59] [CCSD(T)/aug′-cc-pVTZ] were evaluated with CFOUR.[50] Natural bond orbital (NBO) charge analyses[27−29] and c-PCM (Polarizable Continuum Model)[60−65] computations (MP2/DZP++) were carried out with Gaussian 09.[66]

Vertical block-localized wave functions (BLW)[18−20] at the HF/DZP++//CCSD(T)/aug′-cc-pVTZ level were used to compute electron delocalization energies (DE) for the ethyl, propyl, allyl, benzyl, propargyl, and acetonitrile halides [$BLW_{DE(reactant)}$], as well as their S_N2 TSs [$BLW_{DE(TS)}$]. Each BLW_{DE} quantity involves an energy difference between the fully delocalized wave function (Ψ_{Deloc}) of the target system and its artificially localized state (Ψ_{Loc}), in which electron delocalization has been disabled mathematically between the C_α-fragment and substrate π orbitals or the R group (Figure 3). Despite the lack of formal π orbitals, substrates with saturated R groups should be included in BLW analyses because hyperconjugation with the reaction center C_α−F bonds can occur via $\sigma \rightarrow \sigma^*$ orbital interactions. ΔBLW_{DE} estimates the effect of conjugation/hyperconjugation on the computed S_N2 E^b energies. Positive ΔBLW_{DE} values indicate a stabilized TS as compared to the reactant; negative ΔBLW_{DE} values reflect the opposite.

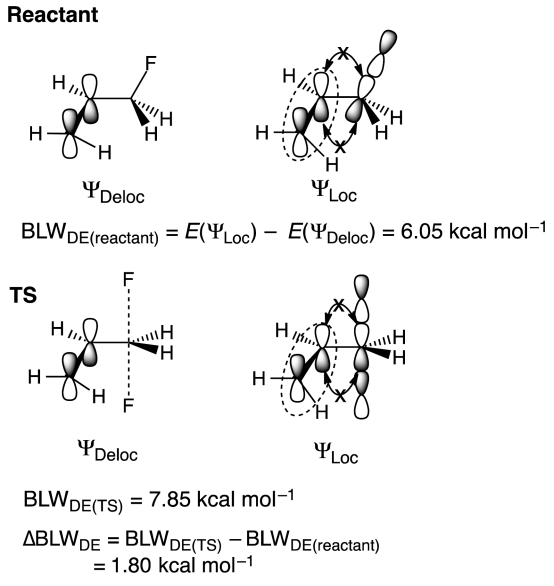

Figure 3. Illustration of the BLW treatment for quantifying electron delocalization between the allyl π orbital and $\sigma(C_\alpha$−F) bonds in allyl fluoride [$BLW_{DE(reactant)}$] and its S_N2 TS [$BLW_{DE(TS)}$]. ΔBLW_{DE} estimates the energetic effect of conjugation on the computed S_N2 E^b energies. Dotted circles show block-localized subspaces; crossed out arrows indicate disabled interactions.

Activation strain (AS) analyses[30,31] were performed with CCSD(T)/aug-cc-pVTZ wave functions. The AS scheme decomposes the E^b energies as the sum of two terms: (1) the energy required to distort the isolated reactant to the geometry it assumes in the TS (ΔE_{strain}), and (2) the interaction energy gained by forming the TS from the nucleophile and strained reactant (ΔE_{int}). Previous work[14] on *p*-benzyl fluoride derivatives found that the ΔE_{strain} term was virtually constant while ΔE_{int} varied greatly and mirrored the intrinsic electrostatic interactions between the nucleophile and substrate.

RESULTS AND DISCUSSION

Focal Point Analyses: Propyl, Allyl, and Propargyl. Our focal-point analyses (Tables 1, 2; Supporting Information, Table S1) of the propyl ($CH_3CH_2CH_2X + X^-$), allyl ($CH_2{=}CHCH_2X + X^-$, **1t** and **2t**), and propargyl ($HC{\equiv}CCH_2X + X^-$) halide (X = F, Cl) S_N2 identity exchange TS energies (E^b) provide strong evidence against the π-conjugation interpretation of the S_N2 allylic effect. These substrates all have a three-carbon skeleton and allow a uniform evaluation of C_α−F bond conjugation with a single set of aligned π orbitals. The computed E^b energies for the coplanar allyl fluoride TS (**1t**, Figure 4) (−0.60) and the propargyl fluoride TS (−3.34) are 0.74 and 3.48 kcal mol^{-1}, respectively, lower than in the propyl fluoride case (+0.14). Likewise, the E^b energies for allyl (+2.54) and propargyl (+2.02) chloride are 0.82 and 1.34 kcal mol^{-1} lower than that of propyl chloride (+3.36). Yet if conjugative effects dominate the rates of these intrinsic S_N2 reactions, why should the propargyl halides display substantially lower E^b energies than their allyl (**1t**) analogues even though only one set of π orbitals is available for delocalization in both cases? Moreover, why should strikingly close E^b energies occur for the two allyl fluoride TS conformations (Figures 4 and 6) with (**1t**, −0.60) and without (**2t**, −0.64) the proper alignment for π-conjugation with the C_α−F bonds? Other important interactions are clearly at work in addition to π-conjugation.[67]

Table 1. Computed High-Level (FPA) E^w, E^*, and E^b Energies (kcal mol^{-1}) and Uncorrelated E^b(HF) Hartree−Fock (CBS) Values for the Propyl, Allyl (1t, 2t), and Propargyl Fluoride/Chloride S_N2 Identity Exchange Reactions[a]

	E^w	E^*	E^b(FPA)	E^b(HF)
propyl−F	−16.48	+16.62	+0.14	+10.36
allyl (**1t**)−F[b]	−19.24	+18.63	−0.60	+11.17
allyl (**2t**)−F[b]	−18.93	+18.29	−0.64	+10.18
propargyl−F	−19.78	+16.44	−3.34	+8.86
propyl−Cl	−12.88	+16.24	+3.36	+10.69
allyl (**1t**)−Cl	−12.98	+15.52	+2.54	+11.48
propargyl−Cl	−12.64	+14.65	+2.02	+12.34

[a]Based on CCSD(T)/aug′-cc-pVTZ reference geometries with MP2/aug′-cc-pVTZ ZPVE corrections included. [b]Computed with respect to the lowest-energy *syn*-periplanar allyl fluoride conformer (**2**).

A remarkable fact from Table 1 is the complete absence of an allylic effect at the HF/CBS limit, which vitiates conventional viewpoints because π-conjugation is an orbital mixing effect that is fully incorporated at the HF level. In fact, for **1t** of both the fluoride and chloride systems, E^b(HF) for the allyl TS is actually higher than that of propyl by about 0.8 kcal mol^{-1}. Without electron correlation, E^b(HF) for the unconjugated TS of **2t** is even lower than that of **1t**.

The two-dimensional FPA layouts in Table 2 show consistent convergence of the E^b values for the fluoride systems toward both the atomic-orbital basis set (vertical) and the electron correlation (horizontal) limits. The aug-cc-pVQZ values are all within 0.3 kcal mol^{-1} of the predicted CBS energies at each level of theory, bolstering confidence in the extrapolations. The correlation increments (δ) are similar in sign and magnitude for all reactions and are remarkably consistent with corresponding statistics found in comprehensive studies of S_N2 reactions.[14,15,24−26] In particular, the high-order δ[CCSD(T)] increments cluster between −3.0 and −3.6

dx.doi.org/10.1021/ja4111946 | J. Am. Chem. Soc. 2014, 136, 3118−3126

Table 2. Focal Point Tables[a] for the Net Activation Barriers (E^b, kcal mol^{-1}) of the Propyl, Allyl (1t, 2t), and Propargyl Fluoride S_N2 Identity Exchange Reactions

	ΔE (HF)	δ (MP2)	δ (CCSD)	δ [CCSD(T)]	ΔE (NET)
(a) $CH_3-CH_2-CH_2F + F^-$					
aug-cc-pVDZ	+7.99	−9.16	+0.99	−2.98	[−3.16]
aug-cc-pVTZ	+10.58	−9.34	+1.24	−3.10	[−0.62]
aug-cc-pVQZ	+10.75	−9.17	+1.38	−3.04	[−0.09]
aug-cc-pV5Z	+10.85	−8.99	[+1.38]	[−3.04]	[+0.19]
CBS limit	[+10.90]	[−8.79]	[+1.38]	[−3.04]	[+0.44]
E^b(FPA) = +0.44 − 0.54 + 0.23 = 0.14 kcal mol^{-1}					
(b) $CH_2{=}CHCH_2F + F^-$ (**1t**, Coplanar)					
aug-cc-pVDZ	+9.11	−11.65	+2.23	−3.48	[−3.79]
aug-cc-pVTZ	+11.60	−11.47	+2.56	−3.63	[−0.93]
aug-cc-pVQZ	+11.73	−11.38	+2.70	−3.59	[−0.53]
aug-cc-pV5Z	+11.83	−11.25	[+2.70]	[−3.59]	[−0.31]
CBS limit	[+11.89]	[−11.19]	[+2.70]	[−3.59]	[−0.11]
E^b(FPA) = −0.11 − 0.73 + 0.25 = −0.60 kcal mol^{-1}					
(c) $CH_2{=}CHCH_2F + F^-$ (**2t**, Perpendicular)					
aug-cc-pVDZ	+7.60	−9.50	+1.20	−3.12	[−3.81]
aug-cc-pVTZ	+10.37	−9.83	+1.45	−3.26	[−1.27]
aug-cc-pVQZ	+10.55	−9.74	+1.58	−3.21	[−0.82]
aug-cc-pV5Z	+10.65	−9.60	[+1.58]	[−3.21]	[−0.58]
CBS limit	[+10.71]	[−9.45]	[+1.58]	[−3.21]	[−0.37]
E^b(FPA) = −0.37 − 0.53 + 0.26 = −0.64 kcal mol^{-1}					
(d) $CH{\equiv}CCH_2F + F^-$					
aug-cc-pVDZ	+6.60	−11.95	+2.59	−3.38	[−6.14]
aug-cc-pVTZ	+9.11	−12.15	+2.89	−3.57	[−3.73]
aug-cc-pVQZ	+9.27	−12.13	+3.01	−3.55	[−3.40]
aug-cc-pV5Z	+9.35	−12.01	[+3.01]	[−3.55]	[−3.20]
CBS limit	[+9.40]	[−11.88]	[+3.01]	[−3.55]	[−3.02]
E^b(FPA) = −3.02 − 0.54 + 0.22 = −3.34 kcal mol^{-1}					

[a] δ denotes computed increments with respect to the preceding level of theory in the hierarchy HF → MP2 → CCSD → CCSD(T). Brackets signify increments obtained from basis set extrapolations or additivity approximations. Each final E^b(FPA) value is the sum of ΔE_{NET}, ΔZPVE[MP2/aug′-cc-pVTZ], and the CCSD(T)/aug-cc-pCVTZ core correlation correction, listed in order; CCSD(T)/aug′-cc-pVTZ reference geometries were used.

kcal mol^{-1}. The FPA tables for the chloride systems (Supporting Information, Table S1) generally exhibit even better convergence than those for the fluoride reactions.

Groundbreaking CCSDT(Q)/aug-cc-pVDZ computations we have executed on the $CH_3X + X^-$ (X = F, Cl) reactions (Supporting Information, Table S2) show that the next increment in the correlation series for E^b should be near −0.3 kcal mol^{-1} for the systems studied here. Thus, our FPA net barriers should be accurate to 0.5 kcal mol^{-1} or better.

Origin of the S_N2 Allylic Effect. Although our detailed analyses of the computed S_N2 net activation barriers (E^b), electrostatic potentials, NBO charges, and ΔBLW_{DE} energies for the ethyl, propyl, methyl, allyl (**1t**, **2t**), benzyl, propargyl, and acetonitrile halide (X = F, Cl) identity exchange reactions show that conjugative and hyperconjugative effects do contribute somewhat to TS lowering, simple electrostatic interactions within the TS are far more important and account for the large range of E^b energies.

The E^b values presented in Tables 3 and 4 from FPA computations on $R-CH_2X + X^-$ (X = F, Cl) S_N2 reactions follow the sequence $R-CH_2$ = ethyl > propyl > methyl ≈ allyl > propargyl > benzyl > acetonitrile. The order of these net barriers generally agrees with the average experimental relative S_N2 reaction rates for propyl, ethyl, methyl, allyl, and benzyl halides (0.4:1:30:40:120) in various organic solvents.[3] There is no clear correlation between the internal barriers E^* and relative rates, in accord with previous work on benzyl halide S_N2 reactions.[14] Note that a clear S_N2 allylic effect is only present when **1t** is compared to ethyl and propyl halides, as opposed to other substrates in the series. While the goal of the current study is to analyze S_N2 intrinsic reactivities unobscured by solvation effects that are often considerable, the qualitative accord found here between gas- and condensed-phase reactivity trends is appealing.

Although the ΔBLW_{DE} (Table 3) values for allyl (**1t**), benzyl, propargyl, and acetonitrile fluoride are all within the 1.65−2.24 kcal mol^{-1} range, their E^b energies vary drastically from −0.60 to −14.98 kcal mol^{-1}! The situation is similar for the analogous chloride series; ΔBLW_{DE} varies by only 1.1 kcal mol^{-1}, whereas the span of E^b values is about 7 times larger. Because the substrates within each series are stabilized by electron delocalization to nearly the same extent, their failure to exhibit similar S_N2 reaction rate enhancements rebuts the claim that π-conjugation plays a decisive role for relative S_N2 reaction rates.[17]

Our computations reveal that intramolecular electrostatic interactions are responsible for the wide range of E^b energies in these systems. At the TS structures of the allyl **1t**, benzyl, propargyl, and acetonitrile fluoride systems, the fluorines exhibit negative NBO charges ranging only from −0.67 to −0.71, but the $Q_{TS}(C_\beta)$ charges vary greatly from −0.15 to +0.35 (Figure 4). The NBO charges of the corresponding chlorides exhibit the same trends. As illustrated in Figure 5, attractive $C_\beta(\delta^+)\cdots X(\delta^-)$ interactions reduce E^b values (faster

dx.doi.org/10.1021/ja4111946 | J. Am. Chem. Soc. 2014, 136, 3118−3126

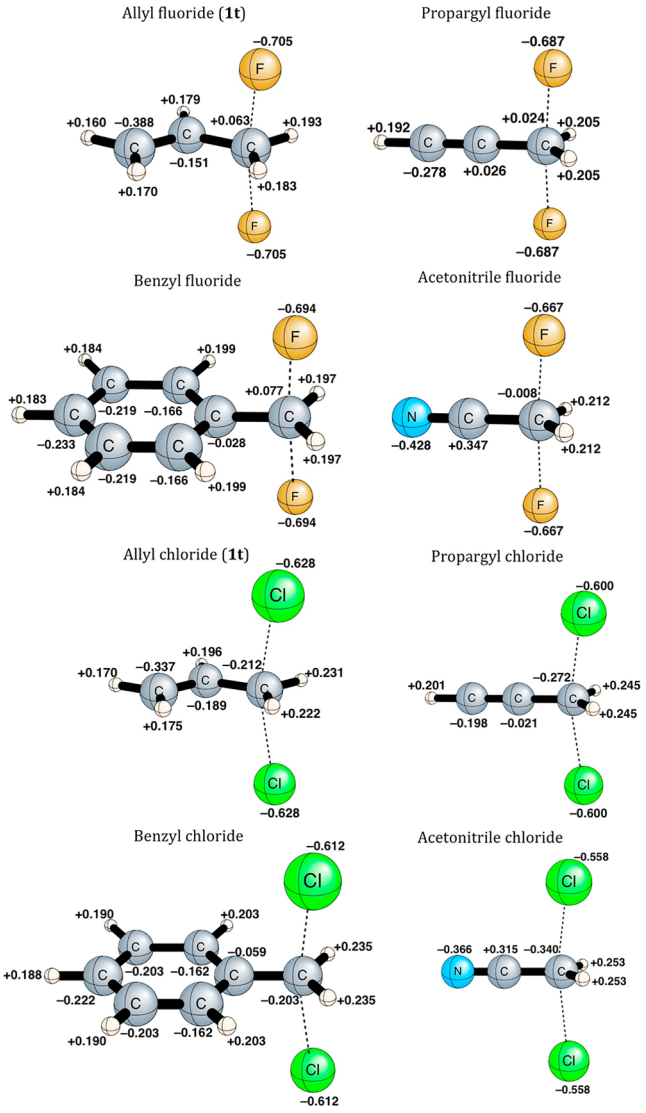

Figure 4. Computed NBO atomic charges (MP2/DZP++) for the allyl **1t**, propargyl, benzyl, and acetonitrile halide (X = F, Cl) TSs.

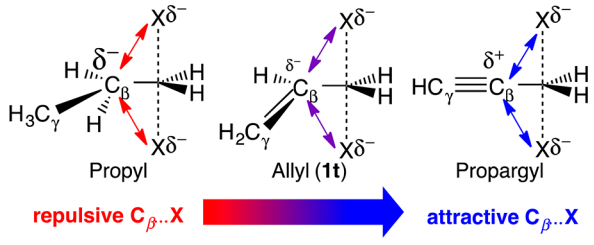

Figure 5. Electrostatic interactions underlying the S_N2 allylic effect. Within a series of analogues, repulsive $C_\beta(\delta^-)\cdots X(\delta^-)$ (red) and attractive $C_\beta(\delta^+)\cdots X(\delta^-)$ (blue) intramolecular interactions (X = F, Cl) in the TS between C_β and the nucleophile (Nu)/leaving groups (LG) retard and enhance S_N2 rates, respectively; purple denotes intermediate interactions.

S_N2 rates), whereas repulsive $C_\beta(\delta^-)\cdots X(\delta^-)$ interactions increase E^b energies (slower S_N2 rates). When the $Q_{TS}(C_\gamma)$ charges are altered substantially by substituents, longer-range $C_\gamma\cdots X$ electrostatic interactions also can be an important influence on E^b. The linear dependence of $Q_{TS}(C_\beta)$ versus E^b for the fluoride series, with a correlation coefficient (r) of 0.979,

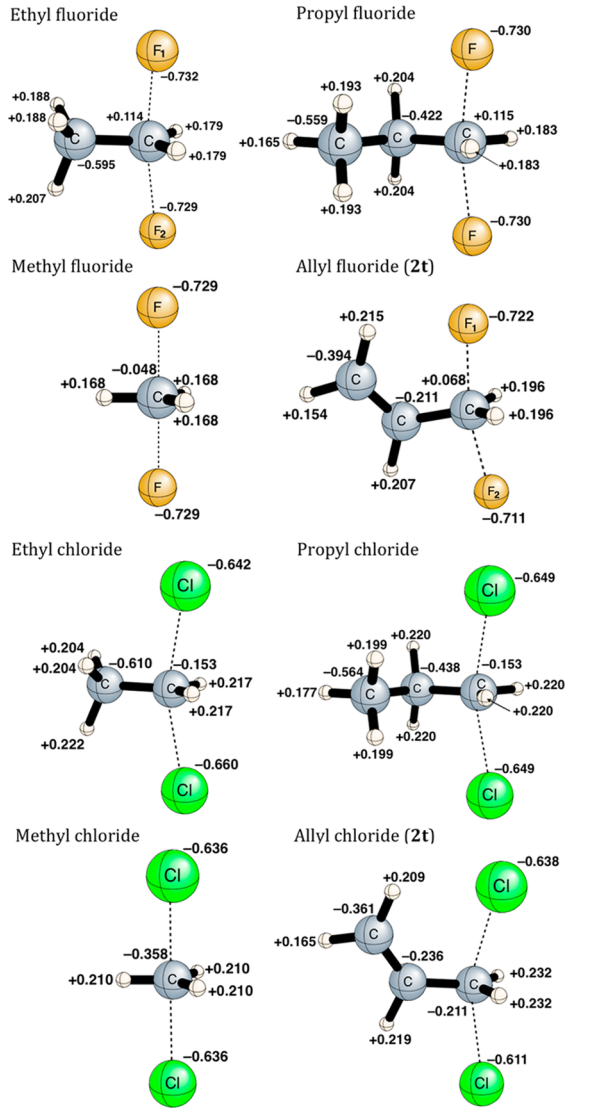

Figure 6. Computed NBO atomic charges (MP2/DZP++) for the allyl **2t**, ethyl, propyl, and methyl halide (X = F, Cl) S_N2 TSs.

substantiates the electrostatic picture. Consistent with this explanation, the more electrostatically stabilized TSs exhibit shorter $d(C_\beta\cdots F)$ distances.

Pearson et al.[68] interpreted the experimentally observed fast S_N2 reaction rates for chloroacetone (10^3 times faster than benzyl chloride) using similar electrostatic arguments. As in chloroacetone, the S_N2 TSs of α—halo carbonyl species are stabilized both by π-conjugation and by attractive electrostatic $C_\beta(\delta^+)\cdots Nu/LG(\delta^-)$ interactions.

In the absence of π-conjugation, the E^b energies of the ethyl, propyl, and allyl **2t** fluoride TSs for S_N2 identity exchange also correlate remarkably well with the $Q_{TS}(C_\beta)$ charges (r = 0.978), as shown in Table 4 and Figure 6. Likewise, the TS $d(C_\beta\cdots F)$ distances follow the order of decreasing Coulombic repulsion between the negatively charged C_β and F atoms. Because hydrogens are more electropositive than carbons, the $Q_{TS}(C_\beta)$ charges become more negative when C_β goes from secondary to primary. Consequently, the net barrier E^b is lower in propyl fluoride than in ethyl fluoride. In methyl fluoride, where a negative C_β is replaced by a positive H, E^b is lower still, at least in part due to attractive $H(\delta^+)\cdots F(\delta^-)$ interactions. The

dx.doi.org/10.1021/ja4111946 | J. Am. Chem. Soc. 2014, 136, 3118−3126

Table 3. Computed E^b Energies (FPA, kcal mol^{-1}), NBO Charges ($Q_{TS}(C_\beta)$, $Q_{TS}(C_\alpha)$, MP2/DZP++), $d(C_\beta\cdots X)$ Distances (Å), and Vertical ΔBLW_{DE} Values (HF/DZP++, kcal mol^{-1}) for the TSs of the Allyl (1t), Benzyl, Propargyl, and Acetonitrile Fluoride and Chloride S_N2 Systems

	allyl (**1t**)	propargyl	benzyl	acetonitrile
X = F				
E^b(FPA)	−0.60	−3.34	−4.63[a]	−14.98
E^*(FPA)	18.64	16.44	18.78[a]	15.00
$Q_{TS}(C_\beta)$	−0.151	+0.026	−0.028	+0.347
$Q_{TS}(C_\alpha)$	+0.063	+0.024	+0.077	−0.008
$d(C_\beta\cdots F)$	2.419	2.387	2.403	2.332
ΔBLW_{DE}	1.80	1.65	2.24	1.88
X = Cl				
E^b(FPA)	+2.54	+2.02	+0.24[a]	−5.11
E^*(FPA)	15.52	12.34	15.02[a]	14.27
$Q_{TS}(C_\beta)$	−0.189	−0.021	−0.059	+0.315
$Q_{TS}(C_\alpha)$	−0.212	−0.272	−0.210	−0.340
$d(C_\beta\cdots Cl)$	2.913	2.883	2.883	2.816
ΔBLW_{DE}	4.18	3.72	3.27	3.05

[a]Reference 14.

Table 4. Computed E^b Energies (FPA, kcal mol^{-1}), NBO Charges ($Q_{TS}(C_\beta)$, $Q_{TS}(C_\alpha)$, MP2/DZP++), $d(C_\beta\cdots X)$ Distances (Å), and Vertical ΔBLW_{DE} Values (HF/DZP++, kcal mol^{-1}) for the TSs of the Ethyl, Propyl, Methyl, and Allyl (2t) Fluoride and Chloride S_N2 Systems

	ethyl	propyl	methyl	allyl (**2t**)[a]
X = F				
E^b(FPA)	+1.50	+0.14	−0.53	−0.64
E^*(FPA)	17.29	16.62	13.04	18.29
$Q_{TS}(C_\beta)$	−0.595	−0.422	(Q_H = +0.168)	−0.211
$Q_{TS}(C_\alpha)$	+0.114	+0.115	−0.048	+0.068
$d(C_\beta\cdots F)$	2.513	2.479		2.439
ΔBLW_{DE}	−2.32	−1.73		−0.63
X = Cl				
E^b(FPA)	+4.64	+3.36	+2.13	
E^*(FPA)	16.78	10.69	12.94	
$Q_{TS}(C_\beta)$	−0.609	−0.438	(Q_H = +0.210)	−0.236
$Q_{TS}(C_\alpha)$	−0.153	−0.153	−0.358	−0.231
$d(C_\beta\cdots Cl)$	3.002	2.962		2.932
ΔBLW_{DE}	−2.66			−0.61

[a]The **2t** structure of allyl chloride is actually a second-order saddle point rather than a genuine S_N2 TS. See the Supporting Information for details.

ΔBLW_{DE} values for ethyl, propyl, and allyl (**2t**) are all negative, indicating greater hyperconjugation in the reactant than in the TS of each S_N2 reaction.

Electron Correlation Effects on S_N2 Barriers. The S_N2 reaction barriers are lowered dramatically by electron correlation, as highlighted in the accompanying FPA tables. In the propyl versus allyl fluoride comparison, the "allylic effect" is entirely an electron correlation phenomenon that only arises beyond the HF/CBS limit. This observation is in accord with an earlier finding[8] that electron correlation is solely responsible for the dramatic stabilization of the S_N2 TS of chloroacetonitrile relative to methyl chloride. Such electron correlation effects can be understood on the basis of changes in the negative charge flow (Q_{flow}, Figure 7) from the nucleophile to the substrate RCH_2 moiety upon formation of the S_N2 TS.

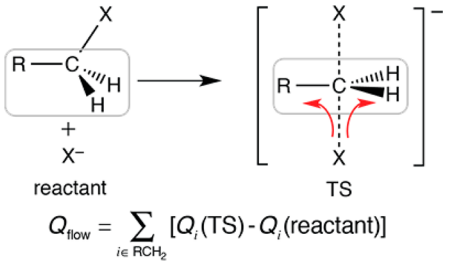

Figure 7. Q_{flow} is the difference between S_N2 TS and reactant values for the sum of NBO charges within the RCH_2 group. This quantity measures the charge transferred from the incoming nucleophile to the substrate upon TS formation.

Specifically, insight is gained by computing ΔQ_{flow} = Q_{flow}(MP2/DZP++) − Q_{flow}(HF/DZP++) as the additional charge flow afforded by electron correlation (Supporting Information, Table S5). Remarkably, the correlation effect on the net barriers, E^b(FPA) − E^b(HF), exhibits a good linear dependence on ΔQ_{flow} for the diverse collection of S_N2 systems considered here (r = 0.941 for fluorides, Figure 8; r = 0.921 for

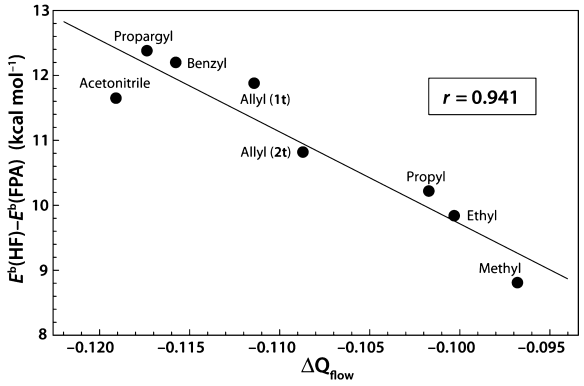

Figure 8. Linear dependence of the S_N2 net barrier reduction due to electron correlation, E^b(HF) − E^b(FPA), on the additional charge flow provided by electron correlation, ΔQ_{flow} = Q_{flow}(MP2/DZP++) − Q_{flow}(HF/DZP++), for several fluoride identity exchange reactions.

chlorides). Unlike π-conjugation, which involves electron delocalization within a single HF electronic configuration, ΔQ_{flow} arises from the influence of excited electronic configurations in the molecular wave functions. While the underlying electronic structure changes are intricate, their overall effect can be understood quite well by a simple electrostatic picture.

Substituent Effects on S_N2 Reactivities. Rigorous computations (Table 5) on substituted allyl fluoride derivatives (**1**−Y, Y−CH=CHCH$_2$F; Y = H, CH$_3$, CH=CH$_2$, C≡CH, CHO, C≡N, OCH$_3$, F, Cl, NO$_2$, Figure 9) yield a striking range of E^b values (+0.56 to −16.81 kcal mol^{-1}) and instructive $Q_{TS}(C_\beta)$ and ΔBLW_{DE} results. For **1**−Y species with a H_δ or C_δ atom (Y = H, CH$_3$, CH=CH$_2$, C≡CH, CHO, C≡N), the NBO charges $Q_{TS}(C_\beta)$ in the TS correlate satisfactorily with the wide E^b variations (r = 0.945), while the corresponding ΔBLW_{DE} values range from only 1.8 to 2.2 kcal mol^{-1} and display a poor correlation with E^b (r = 0.825). Longer-range $C_\gamma\cdots F$ electrostatic interactions also affect the magnitudes of E^b. Thus, when δ-heteroatoms (Y = OCH$_3$, F, Cl, NO$_2$) that engender disparate $Q_{TS}(C_\gamma)$ values (−0.081 to +0.287) are included in the data set, the E^b versus $Q_{TS}(C_\beta)$ correlation

dx.doi.org/10.1021/ja4111946 | J. Am. Chem. Soc. 2014, 136, 3118−3126

Table 5. Computed E^b Energies (FPA, kcal mol^{-1}), Vertical ΔBLW_{DE} Values (HF/DZP++, kcal mol^{-1}), and NBO Charges ($Q_{TS}(C_\beta)$, $Q_{TS}(C_\gamma)$, at MP2/DZP++) for the S_N2 TSs (1t) of Substituted Allyl Fluorides Y−CH═CHCH$_2$F[a]

substituents	E^b (FPA)	E^* (FPA)	ΔBLW_{DE}	$Q_{TS}(C_\beta)$	$Q_{TS}(C_\gamma)$
H	−0.75	18.64	1.80	−0.151	−0.186
CH_3	+0.28	19.59	1.82	−0.166	−0.388
$CH═CH_2$	−3.37	18.40	2.10	−0.112	−0.234
C≡CH	−6.22	19.39	1.95	−0.091	−0.282
CHO	−12.62	14.54	2.07	−0.065	−0.311
C≡N	−14.67	19.92	2.20	−0.066	−0.335
subset correlation with E^b:			r = 0.825	r = 0.945	
δ heteroatoms					
OCH_3	+0.56	21.63	3.30	−0.291	+0.195
F	−3.98	22.43	1.79	−0.258	+0.287
Cl	−6.45	21.75	1.72	−0.181	−0.170
NO_2	−16.81	17.53	3.07	−0.095	−0.081
total correlation with E^b:			r = 0.214	r = 0.681	

[a]Based on CCSD(T)/aug′-cc-pVTZ reference geometries and MP2/aug′-cc-pVTZ ZPVEs. To maintain a consistent comparison, E^b and E^* are computed with respect to the *gauche* conformer of each allyl fluoride reactant that is connected to TS (**1t**) by the S_N2 intrinsic reaction path (IRP), as discussed in the Supporting Information.

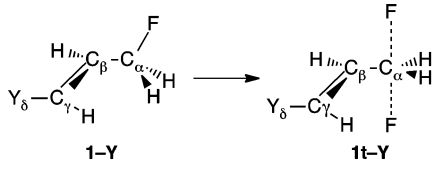

Figure 9. Studied S_N2 reactions of allyl fluoride derivatives.

deteriorates (r = 0.681). The inclusion of such heteroatoms worsens the E^b versus ΔBLW_{DE} correlation (r = 0.214) even more dramatically.

The top panel of Figure 10 shows that the net S_N2 barrier E^b for the ten allyl fluoride (**1t**−Y) systems (Table 5) tracks closely (r = 0.986) with the electrostatic potential (V_{TS}) at C_β in the TS. Less negative $V_{TS}(C_\beta)$ values correspond to lower E^b energies and faster intrinsic S_N2 rates. $V_{TS}(C_\beta)$ is successful as a reactivity descriptor not only for allyl fluoride derivatives but also for propyl and benzyl systems (Table 6; Supporting Information, Tables S6−S9, Figures S4−S7). The activation strain analysis[53,54] (bottom panel of Figure 10; Supporting Information, Tables S12, S13, Figures S8, S9) reveals that the reactivity trends are dominated by the electronic interaction energy ΔE_{int} rather than the substrate distortion energy ΔE_{strain}, and that ΔE_{int} depends linearly on $V_{TS}(C_\beta)$ (r = 0.975). Accordingly, ΔE_{int} and E^b exhibit a strong correlation with one another (r = 0.978), and the AS model provides a link for explaining how the net barriers are governed by intrinsic electrostatics.

Earlier research by Galabov et al.[14,56] found that the electrostatic potential at the reaction center, $V_{TS}(C_\alpha)$, is also a strong indicator of S_N2 reactivity, because it is sensitive to induction by distal substituents. In fact, the $V_{TS}(C_\alpha)$ correlation with E^b is generally superior to that of $V_{TS}(C_\beta)$ (Table 6). The striking predictive capability of both $V_{TS}(C_\alpha)$ and $V_{TS}(C_\beta)$ in an increasingly larger set of systems indicates that the corresponding intrinsic (gas-phase) S_N2 reactivities are determined

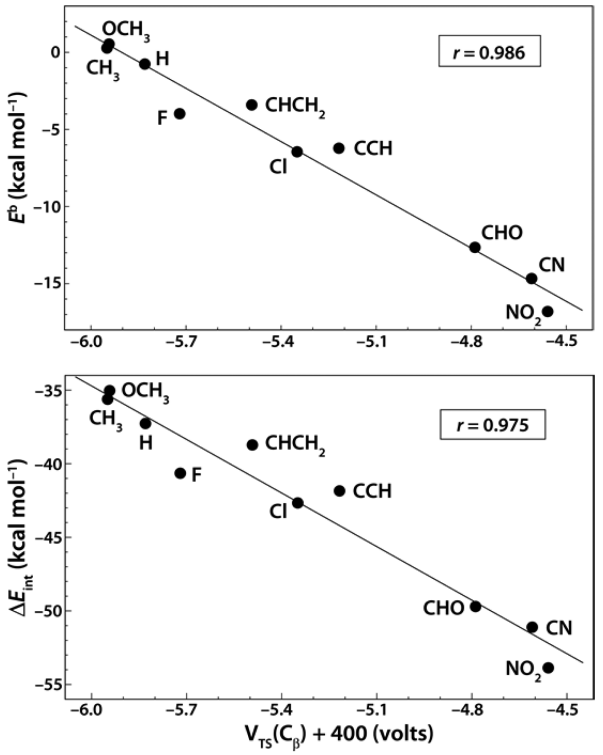

Figure 10. Correlation of S_N2 net barriers (E^b, FPA, top) and AS interaction energies (ΔE_{int}, CCSD(T)/aug-cc-pVTZ, bottom) with the electrostatic potential ($V_{TS}(C_\beta)$, CCSD(T)/aug′-cc-pVTZ) at C_β in the S_N2 TSs (**1t**) of substituted allyl fluoride systems (Y−CH═CH−CH$_2$F + F$^-$; Y = H, F, Cl, CH_3, C≡N, C≡CH, CHO, CH═CH_2, OCH_3, NO_2).

Table 6. Correlation Coefficients[a] for E^b versus the Electrostatic Potential V_{TS} at the C_α and C_β Atoms in S_N2 TSs for Fluoride Identity Exchange[b]

series	allyl (**1t**)[c]	allyl (**2t**)	propyl	benzyl
$V_{TS}(C_\alpha)$	0.984	0.993	0.986	0.998
$V_{TS}(C_\beta)$	0.986	0.937	0.955	0.998

[a]FPA (E^b) and CCSD(T)/aug′-cc-pVTZ (V_{TS}) computations for allyl (**1t**) and (**2t**), and uniform B3LYP/DZP++ for benzyl[14] and propyl. B3LYP/DZP++ somewhat overestimates the E^b barriers but in a highly systematic manner,[15,24] so that correlations with electrostatic potentials are preserved. For example, B3LYP/DZP++ yields r = 0.991 versus the FPA value of 0.986 for the data shown in the top panel of Figure 10. [b]Four series of derivatives are listed: allyl **1t** and **2t** (Y−CH═CHCH$_2$F) and propyl (Y−CH$_2$CH$_2$CH$_2$F) with Y = H, F, Cl, CH_3, CN, CCH, CHO, $CHCH_2$, OCH_3, NO_2, as well as *para*-benzyl[14] (Y′−C_6H_4−CH_2F) with a similar set of groups Y′. [c]See footnote a of Table 5.

inherently by the electrostatic environment near the S_N2 reaction center. Importantly, the presence (allyl(**1t**), benzyl) or absence (allyl(**2t**), propyl) of π-conjugative effects has no consequence on the excellent correlations of E^b with $V_{TS}(C_\alpha)$ and $V_{TS}(C_\beta)$.

Because solvent effects on S_N2 reactions are variable, often large, and governed by diverse types of interactions, the electrostatic interpretation advocated here should be considered the basis of intrinsic S_N2 reactivities arising solely from the electronic structure of the substrate and nucleophile. We have performed preliminary MP2/DZP++ computations using the c-PCM model to qualitatively explore S_N2 reactions in water,

dx.doi.org/10.1021/ja4111946 | J. Am. Chem. Soc. 2014, 136, 3118−3126

ethanol, and acetone for the systems $R-CH_2X + X^-$ ($R-CH_2$ = ethyl, propyl, methyl, allyl (**1t**), allyl (**2t**), benzyl, propargyl, and acetonitrile; X = F, Cl). In accord with earlier studies,[69−71] c-PCM solvation always reduced the gas-phase double-well S_N2 potential (Figure 2) to a unimodal barrier; however, accurate predictions of barrier heights required the combination of explicit microsolvation with embedding in a polarizable continuum. Of greatest significance here, the NBO charges in the S_N2 TSs were only marginally affected by c-PCM solvation, and trends among them were well maintained (Supporting Information, Table S4). This observation bodes well for the utility of the electrostatic interpretation as a fundamental basis for understanding S_N2 reactivities in solution.

CONCLUSIONS

Despite having historical precedence, the conventional π-conjugation explanation of the S_N2 allylic and benzylic effects is specious. While the BLW method indicates that electron delocalization between the $C_\alpha-LG/C_\alpha-Nu$ bonds and substrate π orbitals does stabilize the S_N2 TSs of the allyl (**1t**), benzyl, and propargyl derivatives studied here, the effect is virtually constant for a given halide (X = F or Cl) and fails to explain the large range exhibited by S_N2 barriers. Moreover, the TS for allyl fluoride identity exchange whose conformation (**2t**) turns off π-conjugation is slightly lower than the corresponding TS (**1t**) in which π-conjugation is operative. As compared to the propyl fluoride benchmark, our definitive FPA computations show that the intrinsic allylic effect lowers the net S_N2 barrier by 0.85−0.88 kcal mol^{-1}, regardless of the relative orientation of the π system. Finally, without electron correlation, the allyl (**1t**) TSs actually exhibit an inverse allylic effect, that is, higher HF/CBS barriers. As documented here, for a broad spectrum of S_N2 systems, substrate−nucleophile electrostatic interactions in the TSs rather than π-conjugation are key to determining intrinsic reactivities unaltered by solvation effects.

ASSOCIATED CONTENT

Supporting Information

Complete references for quantum chemistry programs; optimized geometric structures and Cartesian coordinates of all S_N2 stationary points; FPA tables for final S_N2 energetics; conformational energy differences; benchmark CCSDT(Q) correlation increments; S_N2 TS properties; data for substituent effects on S_N2 reactivities; c-PCM solvent effects on atomic charges; and charge flow, electrostatic potential, and activation strain analyses. This material is available free of charge via the Internet at http://pubs.acs.org.

AUTHOR INFORMATION

Corresponding Authors

wdallen@uga.edu
ohtbg@wmail.chem.uni-sofia.bg
judywu@uga.edu

Notes

The authors declare no competing financial interest.

ACKNOWLEDGMENTS

B.G. is thankful for the hospitality of the Center for Computational Chemistry, University of Georgia, where most of the present computations were carried out. This research was supported by the U.S. National Science Foundation, grants CHE-1124885 and CHE-1057466, and by EU grant FP7-REGPOT-2011-1 (project Beyond Everest).

REFERENCES

(1) Bach, R. D.; Coddens, B. A.; Wolber, G. J. *J. Org. Chem.* **1986**, *51*, 1030.
(2) Ingold, C. K. *Structure and Mechanism in Organic Chemistry*, 2nd ed.; Cornell University Press: Ithaca, NY, 1954; p 437.
(3) Streitwieser, A. *Chem. Rev.* **1956**, *56*, 571.
(4) Hatch, L. F.; Chiola, V. *J. Am. Chem. Soc.* **1951**, *73*, 360.
(5) DeWolfe, R. H.; Young, W. G. *Chem. Rev.* **1956**, *56*, 753.
(6) King, J. F.; Tsang, G. T. Y.; Abdel-Malik, M. M.; Payne, N. C. *J. Am. Chem. Soc.* **1985**, *107*, 3224.
(7) Wladkowski, B. D.; Wilbur, J. L.; Brauman, J. I. *J. Am. Chem. Soc.* **1994**, *116*, 2471.
(8) Wladkowski, B. D.; Lim, K. F.; Allen, W. D.; Brauman, J. I. *J. Am. Chem. Soc.* **1992**, *114*, 9136.
(9) Lee, I. C.; Kim, C. K.; Lee, B. S. *J. Comput. Chem.* **1995**, *16*, 1045.
(10) Lee, I. C.; Kim, C. K.; Lee, B. S. *J. Phys. Org. Chem.* **1995**, *8*, 473.
(11) Streitwieser, A.; Jayasree, E. G.; Leung, S. S. H.; Choy, G. S. C. *J. Org. Chem.* **2005**, *70*, 8486.
(12) Ochran, R. A.; Uggerud, E. *Int. J. Mass Spectrom.* **2007**, *265*, 169.
(13) Olmstead, W. N.; Brauman, J. I. *J. Am. Chem. Soc.* **1977**, *99*, 4219.
(14) Galabov, B.; Nikolova, V.; Wilke, J. J.; Schaefer, H. F., III; Allen, W. D. *J. Am. Chem. Soc.* **2008**, *130*, 9887.
(15) Gonzales, J. M.; Allen, W. D.; Schaefer, H. F., III. *J. Phys. Chem. A* **2005**, *109*, 10613.
(16) Gaus, M.; Cui, Q.; Elstner, M. *WIREs Comput. Mol. Sci.* **2013**, doi: 10.1002/wcms.1156.
(17) Rawlings, R. E.; McKerlie, A. K.; Bates, D. J.; Mo, Y.; Karty, J. M. *Eur. J. Org. Chem.* **2012**, *2012*, 5991.
(18) Mo, Y.; Bao, P.; Gao, J. *Phys. Chem. Chem. Phys.* **2011**, *13*, 6760.
(19) Mo, Y.; Gao, J.; Peyerimhoff, S. D. *J. Chem. Phys.* **2000**, *112*, 5530.
(20) Mo, Y.; Song, L.; Lin, Y. *J. Phys. Chem. A* **2007**, *111*, 8291.
(21) Allen, W. D.; East, A. L. L.; Császár, A. G. In *Structure and Conformations of Non-rigid Molecules*; Laane, J.; Dakkouri, M.; van der Veken, B., Oberhammer, H., Eds.; Kluwer: Dordrecht, The Netherlands, 1993; p 343.
(22) Császár, A. G.; Tarczay, G.; Leininger, M. L.; Polyansky, O. L.; Tennyson, J.; Allen, W. D. In *Spectroscopy from Space*; Demaison, K. S., Ed.; Kluwer: Dordrecht, The Netherlands, 2001; p 317.
(23) East, A. L. L.; Allen, W. D. *J. Chem. Phys.* **1993**, *99*, 4638.
(24) Gonzales, J. M.; Cox, R. S.; Brown, S. T.; Allen, W. D.; Schaefer, H. F., III. *J. Phys. Chem. A* **2001**, *105*, 11327.
(25) Gonzales, J. M.; Pak, C.; Cox, R. S.; Allen, W. D.; Schaefer, H. F., III; Csaszar, A. G.; Tarczay, G. *Chem.—Eur. J.* **2003**, *9*, 2173.
(26) Schuurman, M. S.; Muir, S. R.; Allen, W. D.; Schaefer, H. F., III. *J. Chem. Phys.* **2004**, *120*, 11586.
(27) Foster, J. P.; Weinhold, F. *J. Am. Chem. Soc.* **1980**, *102*, 7211.
(28) Reed, A. E.; Weinhold, F. *J. Chem. Phys.* **1983**, *78*, 4066.
(29) Reed, A. E.; Weinstock, R. B.; Weinhold, F. *J. Chem. Phys.* **1985**, *83*, 735.
(30) Bickelhaupt, F. M. *J. Comput. Chem.* **1999**, *20*, 114.
(31) Bickelhaupt, F. M.; Ziegler, T.; Schleyer, P. v. R. *Organometallics* **1995**, *14*, 2288.
(32) Bento, A. P.; Sola, M.; Bickelhaupt, F. M. *J. Chem. Theory Comput.* **2008**, *4*, 929.
(33) Gronert, S. *J. Am. Chem. Soc.* **1991**, *113*, 6041.
(34) Gronert, S. *J. Am. Chem. Soc.* **1993**, *115*, 652.
(35) Rablen, P. R.; McLarney, B. D.; Karlow, B. J.; Schneider, J. E. *J. Org. Chem.* **2014**, *79*, 867.
(36) Wu, X.-P.; Sun, X.-M.; Wei, X.-G.; Ren, Y.; Wong, N.-B.; Li, W.-K. *J. Chem. Theory Comput.* **2009**, *5*, 1597.
(37) Čížek, J. *J. Chem. Phys.* **1966**, *45*, 4256.
(38) Crawford, T. D.; Schaefer, H. F., III. *Rev. Comput. Chem.* **2000**, *14*, 33.
(39) Purvis, G. D.; Bartlett, R. J. *J. Chem. Phys.* **1982**, *76*, 1910.

(40) Raghavachari, K.; Trucks, G. W.; Pople, J. A.; Head-Gordon, M. *Chem. Phys. Lett.* **1989**, *157*, 479.
(41) Scuseria, G. E.; Janssen, C. L.; Schaefer, H. F., III. *J. Chem. Phys.* **1988**, *89*, 7382.
(42) Dunning, T. H., Jr. *J. Chem. Phys.* **1989**, *90*, 1007.
(43) Kendall, R. A.; Dunning, T. H., Jr.; Harrison, R. J. *J. Chem. Phys.* **1992**, *96*, 6796.
(44) Woon, D. E.; Dunning, T. H., Jr. *J. Chem. Phys.* **1993**, *98*, 1358.
(45) Becke, A. D. *J. Chem. Phys.* **1993**, *98*, 5648.
(46) Becke, A. D. *J. Chem. Phys.* **1996**, *104*, 1040.
(47) Lee, C. T.; Yang, W. T.; Parr, R. G. *Phys. Rev. B* **1988**, *37*, 785.
(48) Lee, T. J.; Schaefer, H. F., III. *J. Chem. Phys.* **1985**, *83*, 1784.
(49) Pople, J. A.; Binkley, J. S.; Seeger, R. *Int. J. Quantum Chem., Symp.* **1976**, *10*, 1.
(50) CFOUR, a quantum chemical program package written by J. F. Stanton et al. For the current version, see cfour.de.
(51) MOLPRO, version 2010.1; a package of ab initio programs written by H.-J. Werner et al. For the latest version, see molpro.net.
(52) Woon, D. E.; Dunning, T. H., Jr. *J. Chem. Phys.* **1994**, *100*, 2975.
(53) Feller, D. *J. Chem. Phys.* **1992**, *96*, 6104.
(54) Helgaker, T.; Klopper, W.; Koch, H.; Noga, J. *J. Chem. Phys.* **1997**, *106*, 9639.
(55) *The Massively Parallel Quantum Chemistry Program (MPQC)*, Version 2.3.1; Janssen, C. L., et al., Eds.; Sandia National Laboratories: Livermore, CA, 2004.
(56) Galabov, B.; Ilieva, S.; Koleva, G.; Allen, W. D.; Schaefer, H. F., III; Schleyer, P. v. R. *WIREs Comput. Mol. Sci.* **2013**, *3*, 37.
(57) Johnson, B. G.; Gill, P. M. W.; Pople, J. A.; Fox, D. J. *Chem. Phys. Lett.* **1993**, *206*, 239.
(58) Politzer, P. In *Chemical Applications of Atomic and Molecular Electrostatic Potentials: Reactivity, Structure, Scattering, and Energetics of Organic, Inorganic, and Biological Systems*; Politzer, P., Truhlar, D. G., Eds.; Plenum Press: New York, 1981; p 7.
(59) Wilson, E. B. *J. Chem. Phys.* **1962**, *36*, 2232.
(60) Cossi, M.; Barone, V. *J. Chem. Phys.* **2000**, *112*, 2427.
(61) Cossi, M.; Rega, N.; Scalmani, G.; Barone, V. *J. Chem. Phys.* **2001**, *114*, 5691.
(62) Cossi, M.; Rega, N.; Scalmani, G.; Barone, V. *J. Comput. Chem.* **2003**, *24*, 669.
(63) Cossi, M.; Scalmani, G.; Rega, N.; Barone, V. *J. Chem. Phys.* **2002**, *117*, 43.
(64) Scalmani, G.; Frisch, M. J. *J. Chem. Phys.* **2010**, *132*, 114110.
(65) Tomasi, J.; Mennucci, B.; Cammi, R. *Chem. Rev.* **2005**, *105*, 2999.
(66) Frisch, M. J.; et al. *Gaussian 09*, revision D.01; Gaussian, Inc.: Wallingford, CT, 2009.
(67) Allyl fluoride **2t** benefits from two favorable intramolecular H(δ^+)···F(δ^-) hydrogen-bonding interactions that compensate for the loss of π-conjugation. In benzyl fluoride, these electrostatic interactions are much weaker, so that the **2t** analogue is actually a second-order saddle point lying 4.2 kcal mol^{-1} higher in energy than the **1t** transition state (CCSD(T)/aug′-cc-pVTZ//MP2/DZP++). See the Supporting Information for documentation and discussion of the competition between **1t** and **2t** conformations.
(68) Pearson, R. G.; Langer, S. H.; Williams, F. V.; McGuire, W. J. *J. Am. Chem. Soc.* **1952**, *74*, 5130.
(69) Chandrasekhar, J.; Smith, S. F.; Jorgensen, W. L. *J. Am. Chem. Soc.* **1985**, *107*, 154.
(70) Kormos, B. L.; Cramer, C. J. *J. Org. Chem.* **2003**, *68*, 6375.
(71) Vayner, G.; Houk, K.; Jorgensen, W. L.; Brauman, J. I. *J. Am. Chem. Soc.* **2004**, *126*, 9054.